J. Chem. Soc., Faraday Trans. 1, 1981, 77, 2777-2801

Kinetic Studies of Secondary Alcohol Photo-oxidation on ZnO and TiO_2 at 348 K Studied by Gas-chromatographic Analysis

BY JOSEPH CUNNINGHAM* AND BENJAMIN K. HODNETT
Department of Chemistry, University College, Cork, Ireland

Received 3rd *December*, 1980

Kinetics of conversion of propan-2-ol and butan-2-ol to the corresponding ketones by photoassisted dehydrogenation, $(-H_2)^*$, to lower aldehydes by a photoassisted C_α—C_β bond cleavage process, $(\alpha\text{-}\beta)^*$, and to trace quantities of alkene by photoassisted dehydration $(-H_2O)^*$ have been investigated at oxygen partial pressures in the range 0-700 Torr and at alcohol partial pressures of 0-60 Torr, utilising dynamic flow photoreactors and gas-chromatographic analysis. Qualitatively similar results were obtained either with a 'continuous reactant flow plus continuous u.v. illumination' procedure allied to intermittent sampling, or with a 'pulsed reactant and analysis' procedure. Both procedures yielded dependence upon alcohol pressure indicative of two parallel photoassisted pathways to $(-H_2)^*$ product, one being Langmuir–Hinshelwood (LH*) and the other Eley–Rideal (ER*) in character. A decline in activity of the metal oxide surfaces as photoassisted conversion of alcohol increased was observed with both procedures and affected the LH* process for $(-H_2)^*$ more strongly. It is proposed that this LH* process involved alcohol chemisorption and hole localisation at coordinatively unsaturated O^{2-}_{cus} ions. The ER* process is envisaged to have involved encounter of alcohol (from the gas phase or from a reversibly adsorbed weakly bound state) with a much more numerous type of surface location capable of being photoactivated by hole capture. The proposed mechanisms account for observed dependences of the $(-H_2)^*$ process upon square root of the incident light intensity, upon alcohol pressure and upon oxygen pressure.

The work described in this paper on kinetic aspects of the photo-oxidation of alcohols over ZnO and TiO_2, and in a subsequent paper on competitive adsorption aspects of this photocatalytic process over ZnO,[1] involves the application of gas chromatographic analytical procedures to study new or enhanced oxidation reactions which occur at the metal oxide surface upon u.v. illumination of (alcohol vapour + O_2)/metal oxide interfaces. For reasons of experimental convenience, the procedures adopted for many of the studies already published on photoassisted reactions at such interfaces[2-8] have involved an initial pre-exposure of alcohol vapour to the metal oxide surface in the dark, prior to initiation of photo-oxidations such as photodehydrogenation, $(-H_2)^*$, photodehydration, $(-H_2O)^*$, or photoassisted cleavage of the C_α—C_β bond of the parent alcohol, $(\alpha\text{-}\beta)^*$. During such pre-exposure an important role of the undisturbed Lewis acid–base properties (*i.e.* undisturbed by u.v. illumination) has been envisaged in determining relative extents of coverage of the surface by alkoxide,[9] alcoholate[10] or hydrogen-bonded alcohol species.[11] Subsequent incidence of a flux of near-u.v. photons, having energies greater than the band-gap (*ca.* 3.0 eV) of either TiO_2 or ZnO, has been shown by several research groups to bring about continuous evolution of aldehyde and ketone photoproducts from the metal oxide surfaces[2,4-6] corresponding to selective partial oxidation of the alcohol originally absorbed. It is generally agreed that necessary conditions for the continuation of such heterogeneous photo-oxidations to large numbers of molecules converted per adsorption site include the need for simultaneous presence at the interface of near-u.v. photons, metal oxide, vapour phase alcohol and gaseous oxygen. The majority of such studies have been made with a continuous flow of alcohol vapour (2-100 Torr), gaseous oxygen (0-700 Torr) and inert carrier gas over the illuminated metal oxide and have utilised gas-chromatographic techniques for identification and measurements of the products of selective photo-oxidation.[3-5] In addition to extending such g.c. studies in conditions of 'continuous reactant flow', the present work includes studies with a pulsed reactant technique, in which the metal oxide surface was exposed to pulses of premixed (alcohol + O_2) reactant. Variations in efficiency of conversion with amount of alcohol converted per surface site and with amount of reactant in each pulse are readily studied by this technique.

Note, however, that the reactant pressures utilised in this and other g.c. studies are typically one to three orders of magnitude greater than those to which TiO_2 photocatalysts were exposed during studies recently published from these laboratories on mass spectrometric (m.s.) characterization of rutile-catalysed alcohol photo-oxidation.[12] Those m.s. studies gave evidence that holes trapped at co-ordinatively unsaturated oxide ions (*i.e.* O^-_{cus}) on preoxidised TiO_2 surfaces played a dominant role in photo-oxidation of preadsorbed alcohol species, with the result that such photo-oxidations corresponded to photoassisted Langmuir–Hinshelwood-type processes, which shall be denoted in the text by LH*. However, it must be borne in mind in any comparison with the previous work, that the large increases from low reactant pressures characteristic of m.s. work to the greater pressures of the present g.c. study open up possibilities for greater variety in photoassisted surface reactions. For example, the presence of a greatly enhanced pressure of reactant alcohol or oxygen in the gas phase over an illuminated metal oxide should enhance possibilities for interactions between a photoactivated surface lattice species, such as O^{-*}_{cus}, and a reactant species encountering it during its lifetime by direct encounter from the gas phase or whilst in a physisorbed state (*i.e.* photoinitiated versions of an Eley–Rideal or a van der Waals–chemisorbed-type process, which shall both here be denoted by ER*). Kinetic analysis of the photoassisted reactions in g.c. conditions are presented in the present paper in attempts to distinguish contributions by any such photoassisted LH* and ER* processes. An asterisk is used throughout the text to indicate processes and interfaces observed under excitation by photons of energies greater than the band-gap of the ZnO or TiO_2 catalysts.

EXPERIMENTAL

PHOTOCATALYTIC REACTORS

A photocatalytic reactor, developed[3] and kindly supplied by Teichner's group in Lyon, was utilised for experiments with continuous flow of premixed (alcohol + O_2 + N_2) at a total pressure of *ca.* 1 atm and, unless otherwise stated, at a total gas flow rate of 40 $cm^3\ min^{-1}$, over the powdered catalysts (usually 20-500 mg of the oxide materials was deposited as a thin uniform layer on Whatman GF/C permeable membrane). The membrane assembly was sealed across the gas flow direction by Viton 'O' ring seals thus ensuring good contact between oxide catalyst and gas-phase reactants. The reactor was operated by 348 K, unless otherwise stated. The gas flow pattern shown in fig. 1 (*a*), in which all piping was constructed of $\frac{1}{4}$ inch stainless-steel piping which was heated to 300 K throughout to prevent condensation of alcohol vapour, was utilised for studies in the continuous reactant flow mode of operation. Analysis of the gas phase over the metal oxide catalysts was achieved by periodic sampling to a Pye Unicam Series 104 gas chromatograph which was used to achieve separation of reactants and products on a 5 foot long glass column of $\frac{1}{4}$ inch diameter packed with chromosorb 103 (80-100 mesh) held at 400 K at a carrier-gas flow rate of 40 $cm^3\ min^{-1}$. A flame ionization detector (f.i.d.) operating within its region of linear response, as determined by calibration plots, allowed quantitative determination of any hydrocarbon photoproducts.

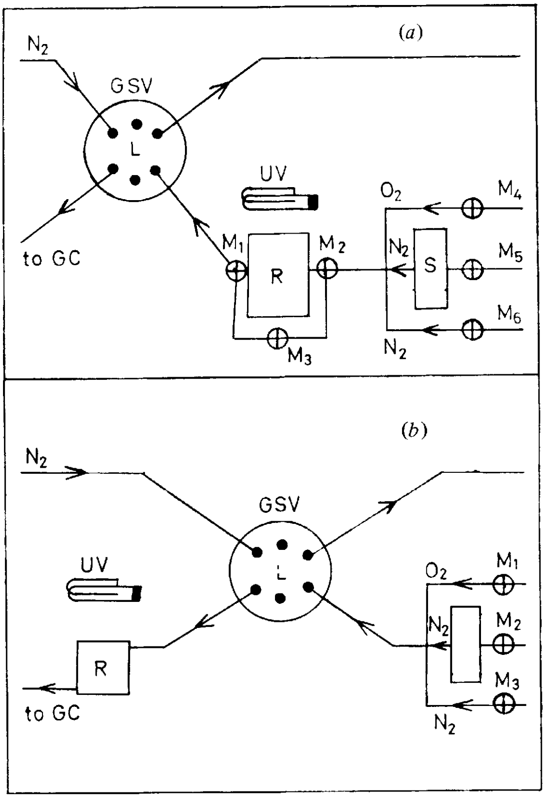

FIG. 1.—Gas flow patterns for (*a*) continuous reactant flow and (*b*) pulsed reactant flow procedures. R, reactor; GSV, gas sampling valve; UV, u.v. source; S, alcohol vapour saturator; M, metal valves; L, gas sampling loop.

Fig. 1 (*b*) illustrates an alternative gas flow pattern in which powdered ZnO or TiO_2 catalyst samples (50-500 mg), held at 348 K, were maintained in a flow of pure carrier gas (flow rate = 55 cm^3 min^{-1}) and positioned immediately before the column of the g.c. system. Pulses of reactant gases (volume of pulse = 0.5 cm^3) were injected periodically into the carrier-gas stream of the g.c. system with the aid of a Pye Unicam gas sampling valve. Thus, the reactant pulse was directed over the metal oxide and, after desorption from the catalyst, gases eluted from the reactor were swept directly onto the column of the chromatograph to be resolved into their component peaks. The Lyon photoreactor was used in this mode of operation for samples preconditioned at temperatures $\leqslant$ 348 K. Reactor design did not however allow for prior high-temperature outgassing of catalyst samples and experiments which required such pretreatment of the oxide samples were carried out with an all-quartz photoreactor into which was sealed a sintered quartz disc on which the powdered metal oxides were usually deposited. Temperature programmed heating of the column, which was the same as that used for the continuous reactant flow mode of operation (*viz.* at 333 K for 4 min followed by a temperature rise of 8 K min^{-1} to 423 K), was necessary to maximise resolution of the g.c. peaks in this mode. Any diminution in alcohol pressure experienced in one pass of the reactant pulse through the reactors, whether caused by adsorption of the alcohol or its photo-oxidation, could be detected with much greater sensitivity in this pulsed reactant mode. Furthermore the initial stages of photoassisted conversions could be examined in detail at low and precisely known exposures of the surface to alcohol and to u.v. illumination.

ILLUMINATION

One of two Hg vapour lamps with small emitting volumes and maxima at 366, 404 and 547 nm in their emissions and weaker maxima at 254, 303 and 333 mn were used in this work, *viz.* a Hanau 125 W medium pressure Hg arc inside a Pyrex water-cooled jacket and a Hanovia 200 W high pressure Hg–Xe arc. For the 'continuous reactant flow' mode of operation, illumination by radiation of selected wavelength and known intensity was maintained without interruption for up to 4 h after its initiation. In order to avoid undesirable photoreduction of the metal oxide surfaces when an oxygen pulse was not in transit, the duration of illumination for the 'pulsed reactant' mode was made comparable to the transit time of the oxygen component of the reactant pulse through the photoreactor. U.v. output of the lamps was routinely monitored by appropriately filtered silicon photocells (U.V. Products, Black Ray Meter) and was transmitted into the photoreactors by appropriate quartz lenses. Several mm thickness of Pyrex were used to prevent wavelengths < 300 nm from entering the photoreactor and intensity was varied by changing the distance between lamps and sample. Potassium ferrioxolate actinometer solutions, in Pyrex containers similar in size and dimension to the photoreactors and placed at the sample position, were used for quantitative determination of photon flux, and this quantity will be expressed below in terms of the number of photons entering the appropriate photoreactor per second. When wavelength dependence of photoassisted reaction was being evaluated, Zeiss narrow-band-pass filters were used to transmit photons centred on 366, 404, 437 or 547 nm and it was invariably found that no photoreaction occurred with the latter two wavelengths.

MATERIALS

All measurements on TiO_2 surfaces were made with high purity, chloride-free, rutile material supplied by New Jersey Zinc Co. and having a specific surface area of 5 $m^2\ g^{-1}$ (code MR-128). A high purity ZnO powder of specific surface area 4 $m^2\ g^{-1}$, supplied under the code SP-500 by New Jersey Zinc Co., was used for all ZnO experiments. For experiments in the 'continuous reactant flow' mode in the Lyon photoreactor these materials were used as supplied, except for several hours outgassing at 348 K in a pure N_2 flow prior to photoreactions. In cases where more rigorous outgassing and pretreatment was necessary, *e.g.* in testing the effects of CO_2 preadsorption, the metal oxide was pretreated in the all-quartz photocatalytic reactor at 623 K in a flow of pure N_2 gas (for a prereduced surface) or of pure O_2 (for a preoxidised surface). Propan-2-ol was AristaR and butan-2-ol A.R. grade and the desired pressure of these alcohols was incorporated into the flow of reactor feed-gas by passing part or all of the gas flow through a column of Linde molecular sieve (type 3 A) which had been previously impregnated with the liquid alcohol at room temperature, following outgassing of the sieve at 600 K. Control of the alcohol vapour pressure was achieved by varying the temperature of a thermostatted jacket around the alcohol-impregnated molecular sieve. Appropriate valves and flow meters allowed introduction of oxygen at selected partial pressures in the range 0-740 Torr, within the constraint that $(P_{N_2}+P_{O_2}+P_{ROH}) \approx 1$ atm.

RESULTS

(1) CONTINUOUS REACTANT FLOW PROCEDURE

(1*a*) GENERAL FEATURES OF SECONDARY ALCOHOL PHOTO-OXIDATION

Fig. 2 summarises results typical of those obtained over TiO_2 by use of the Lyon-type photoreactor in the continuous reactant flow mode of operation. The oxide surface was pre-equilibrated for 1 h at 348 K in the dark with a continuous flow of (alcohol $+ O_2 + N_2$) with partial pressures of 8, 380 and 372 Torr, respectively, prior to commencing continuous illumination by photons of $\lambda > 300$ nm at $t = 0$. Injection of a sample of effluent gases from the photoreactor were made onto the g.c. column after the illumination times indicated on fig. 2. For (butan-2-ol $+ O_2$)/TiO_2* systems, analysis of such samples with the f.i.d. invariably led to time profiles similar to those

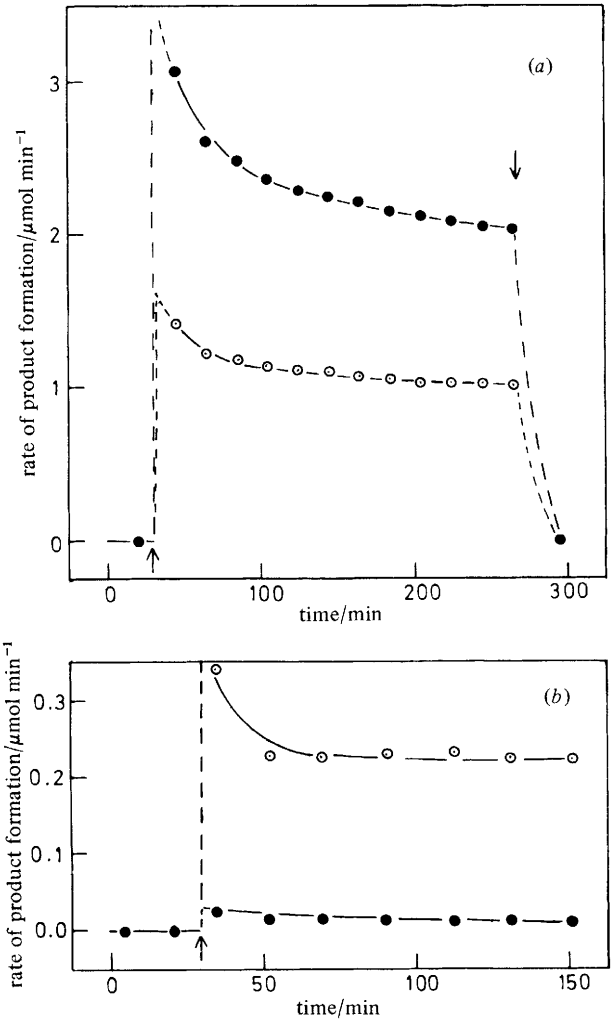

FIG. 2.—(*a*) Time profiles for rates of photoassisted production of butanone (○) and acetaldehyde (●) from butan-2-ol on TiO_2 (MR-128). Arrows indicate start and finish of continuous u.v. illumination. Mass of TiO_2 in reactor (M) = 95 mg; P_{O_2} = 380 Torr, $P_{\text{butan-2-ol}}$ = 8 Torr. (*b*) Time profiles for rate of photoassisted production of acetone (○) and acetaldehyde (●) from propan-2-ol on TiO_2 (MR-128). M = 100 mg, $P_{\text{propan-2-ol}}$ = 8 Torr, P_{O_2} = 380 Torr.

in fig. 2(*a*) for extent of photoassisted conversion to butanone, acetaldehyde, ethanol and propanal. The relative abundances of these detected hydrocarbon photoproducts indicated only dehydrogenation, $(-H_2)^*$, and C_α—C_β bond cleavage, $(\alpha\text{–}\beta)^*$, as comparably efficient photoassisted elimination reactions from the (butan-2-ol + O_2)/TiO_2^* interface in these conditions. Photoassisted dehydrogenation of propan-2-ol to acetone was the dominant product over TiO_2, as illustrated by fig. 2(*b*), which also shows acetaldehyde as a less favoured photoproduct, corresponding to $(\alpha\text{–}\beta)^*$ bond cleavage. Trace quantities of propene were also detected. It is clear from these plots that a fully adequate description of the photoassisted surface processes should account not only for the $(-H_2)^*$ ketone products but also for the $(\alpha-\beta)^*$ product.

The time profile illustrated in fig. 2 for extent of the photoassisted conversion of secondary alcohols to photoproducts [with an initial maximum conversion at the shortest feasible time for reproducible illumination and sampling in this mode of operation (*ca.* 5 min) and a subsequent slow decline towards a photodynamic equilibrium (p.d.eq.) characterised by an apparently constant conversion] was observed in all experiments carried out at high u.v. illumination intensities in the present study. Persistent efforts were made to eliminate the observed decay by varying the flow rate or pretreatments given to the oxides in the dark or the conditions during illumination, but without success. Similar effects had been briefly mentioned by earlier workers who usually chose to utilise as a measure of reproducible photocatalytic activity the constant conversion ultimately attained after the initial decay.

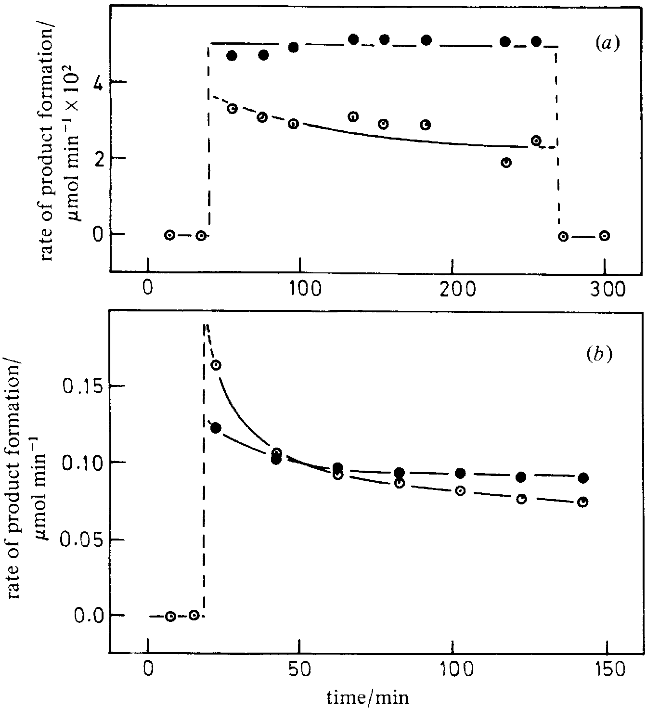

FIG. 3.—Time profiles for rates of photoassisted production of butanone (○) and acetaldehyde (●) from butan-2-ol on ZnO (SP-500). $M = 50$ mg, $P_{\text{butan-2-ol}} = 8$ Torr, $P_{O_2} = 380$ Torr. (*b*) Time profiles for rates of photoassisted production of acetone (○) and acetaldehyde (●) from propan-2-ol on ZnO (SP-500). $M = 200$ mg, $P_{\text{propan-2-ol}} = 20$ Torr, $P_{O_2} = 380$ Torr.

Fig. 3(*a*) and (*b*) show, respectively, time profiles for rates of photoassisted production of butanone and acetaldehyde from a u.v. illuminated (butan-2-ol $+ O_2$)/ZnO* interface and for rates of photoassisted production of acetone and acetaldehyde from a u.v. illuminated (propan-2-ol $+ O_2$)/ZnO* interface. Similar decay in catalytic activity to that reported above for TiO_2 samples is evident for $(-H_2)^*$ over ZnO. It was decided, in view of the magnitude of this decline in extent of conversion and of its important implications for the development of satisfactory models for the $(-H_2)^*$-type photocatalytic activity of the $(O_2 + \text{alcohol})/ZnO^*$ interfaces, that it should be studied by a pulsed reactant technique. Prior to those studies, the dependences of photoassisted conversion upon reactor loading [*cf.* fig. 4(*a*)], upon reactor temperature [*cf.* fig. 4(*b*)] and upon reactant pressures (fig. 5 and 6) were determined in conditions of continuous reactant flow for the systems (butan-2-ol$+O_2$)/TiO_2^* and (propan-2-ol$+O_2$)/ZnO^*.

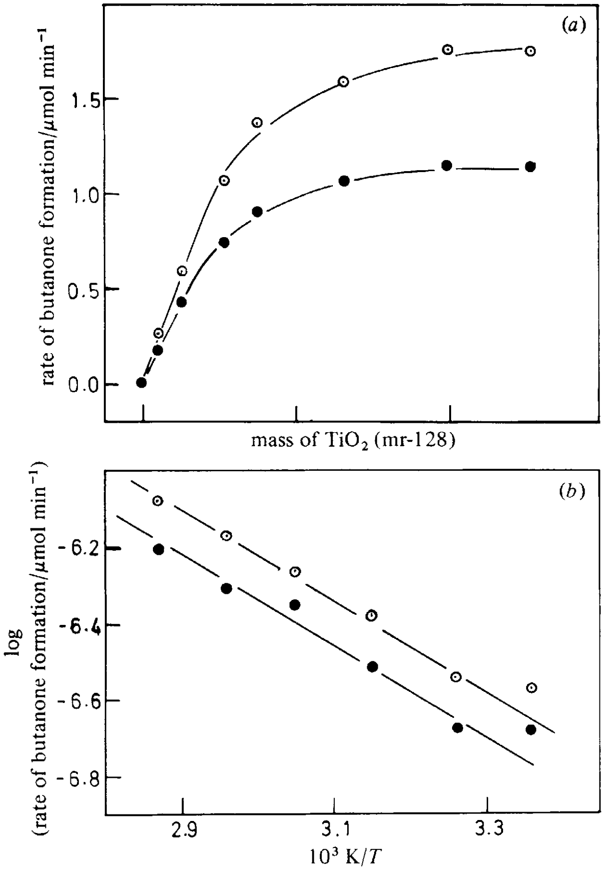

FIG. 4.—(*a*) Influence of the mass of TiO_2 (MR-128) present in the photoreactor on rate of photoassisted production of butanone from butan-2-ol measured after 15 (○) and 115 (●) min u.v. illumination. $P_{\text{butano-2-ol}} = 8$ Torr, $P_{O_2} = 380$ Torr. (*b*) Arrhenius plots for rate of photoassisted production of butanone from butan-2-ol on TiO_2 measured after 15 (○) and 115 (●) min u.v. illumination. $M = 50$ mg, $P_{\text{butan-2-ol}} = 8$ Torr, $P_{O_2} = 380$ Torr.

When the mass of catalyst (TiO_2) present in the photoreactor was varied over the range 20-500 mg, an initial decline in extent of conversion with duration of illumination was observed for all reactor loadings studied. Comparison of the extent of conversion of butan-2-ol to butanone induced after 15 and 115 min u.v. illumination for different reactor loadings is made in fig. 4(*a*) and reveals non-linear dependence upon mass of catalyst. Similar behaviour has been reported by Teichner *et al.*[13] for selective photocatalytic oxidation of alkanes on TiO_2 and explained in terms of a critical thickness of catalyst bed beyond which catalyst particles not located in upper layers were no longer accessible to u.v. illumination. Plots of extent of butan-2-ol conversion to acetaldehyde product exhibited similar behaviour to that outlined for butanone product. Investigations of differing temperatures in the range 300-360 K all demonstrated a persistence of declining catalytic efficiency as conversion increased in conditions of continuous reactant flow for all reaction products. Fig. 4(*b*) shows that linear Arrhenius-type plots of log [rate $(-H_2)^*$] and log [rate $(\alpha\text{-}\beta)^*$] against $1/T$ for these data, measured at set times after commencement of u.v. illumination, yielded apparent activation energies of 21 and 26.5 kJ mol^{-1}, respectively, for these photoassisted processes. The values of these apparent activation energies did not vary significantly with times of illumination between 15 and 115 min, in which time period the activity of the system would normally have changed from a high initial level to a level close to that which pertained at p.d.eq. Thus it appeared that, independent of whether or not the system was at p.d.eq. and despite the observation that rate of photoassisted catalytic conversion of parent alcohol to product aldehydes and ketones on ZnO or TiO_2 diminished as these reactions proceeded, nevertheless reasonable activation energy parameters could be deduced provided that the reaction rates were measured at set times after commencement of illumination.

(1*b*) KINETIC STUDY OF THE PHOTOASSISTED OXIDATION OF PROPAN-2-OL ON ZnO IN THE CONTINUOUS ILLUMINATION, CONTINUOUS REACTANT FLOW MODE OF OPERATION

The system (propan-2-ol + O_2)/ZnO* was chosen for detailed study to evaluate the kinetic parameters which govern this heterogeneous photo-oxidation reaction. As mentioned above, acetone and acetaldehyde were the major photoproducts observed, with trace amounts of propene and methanol also detected, but no reaction was observed in the absence of u.v. illumination or of ZnO. The rates of formation of all products decayed to zero instantaneously when u.v. illumination was stopped. Slow decay in the rates of acetone and acetaldehyde photoproduction as a function of time of u.v. illumination [as shown in fig. 3(*b*)] was observed for all partial oxygen pressures studied in the range 0-740 Torr and for all partial alcohol pressures in the range 0.5-60 Torr. A study of the contact-time dependence of rates of photoassisted production of acetaldehyde and acetone on ZnO indicated that the system was free of diffusional limitations in the standard conditions of this study.

The effect of partial pressure of oxygen on the rate of acetone photoproduction from propan-2-ol on ZnO is outlined in fig. 5. The observed decay in photoassisted conversion to acetone as a function of the time of u.v. illumination (*cf.* fig. 3) imposed the constraint that only conversions measured at identical times after commencement of irradiation under differing P_{O_2} should be compared. Reaction rates measured after 5 or 125 min u.v. illumination with a constant alcohol partial pressure of 20 Torr, a total gas flow rate of 40 cm^3 min^{-1} and a constant intensity of u.v. illumination, are shown in fig. 5. The effect of oxygen partial pressure on conversions at times intermediate between 5 and 125 min u.v. illumination showed similar behaviour to those outlined in fig. 5. The conversion to acetone product measured after 5 min illumination passed through a maximum corresponding to a partial oxygen pressure of *ca.* 400 Torr. At partial oxygen pressures above this value a fall-off in reaction rate was observed [*cf.* fig. 5, curve (i)].

Occurrence of the maxima shown by the experimental data in fig. 5 could qualitatively be accounted for on the basis that some competition for adsorption sites existed between alcohol-related and oxygen-related species. The shift of the maximum rate after 125 min illumination towards $P_{O_2} \approx 600$ Torr would be consistent with an increase in surface coverage by alcohol-related species at the expense of coverage by oxygen-related species.

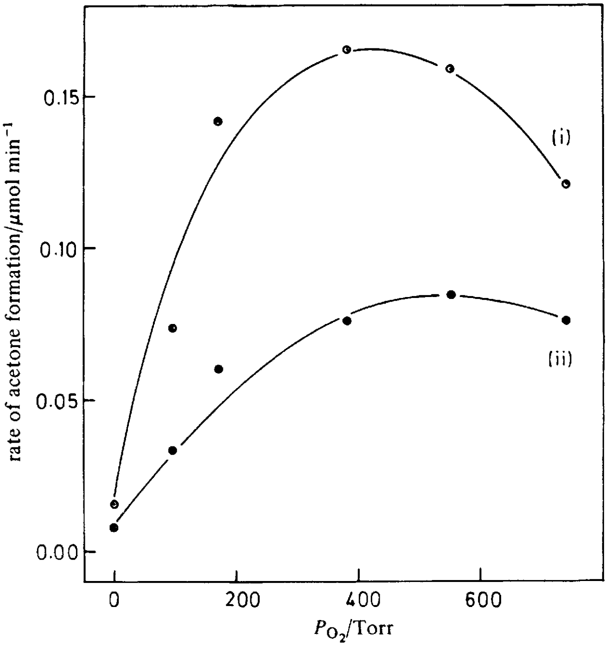

FIG. 5.—Influence of partial oxygen pressure on rate of acetone production from propan-2-ol on ZnO measured after: (i) 5 and (ii) 125 min u.v. illumination. $M = 200$ mg, $P_{\text{propan-2-ol}} = 20$ Torr, $F = 40$ cm^3 min^{-1}.

The question of whether non-dissociatively adsorbed oxygen species or dissociatively chemisorbed oxygen species were involved in photoassisted conversion to acetone was examined for data at oxygen pressures below the maximum in fig. 5 by a least squares analysis of the fit of data for (rate after 125 min illumination) at various values of P_{O_2} to

$$P_{O_2}^n/\text{rate} = a + bP_{O_2}^n. \tag{1}$$

Eqn (1) with $n = \frac{1}{2}$ or $n = 1$ corresponds to the Langmuir equation for adsorption of oxygen with or without dissociation, respectively. Least mean square regression coefficients were 0.984 and 0.510 for $n = 1$ and $n = \frac{1}{2}$, respectively, thereby favouring involvement of non-dissociatively adsorbed oxygen in the mechanism leading to $(-H_2)^*$.

The influence of partial pressure of oxygen upon rate of photoassisted production of acetaldehyde from propan-2-ol on ZnO, at a constant propan-2-ol partial pressure of 20 Torr, was also examined within the framework of data presented in fig. 3-5, *i.e.* that only reaction rates measured at identical times after commencement of u.v. illumination were directly compared for various values of P_{O_2}. The rate of production of acetaldehyde from this system exhibited similar behaviour to that reported in fig. 5 for the analogous acetone product, except that the maxima in reaction rate as a function of P_{O_2} occurred at values of 300-600 Torr and were not as pronounced as in the former case. Additional analysis of these data according to eqn (1) indicated that adsorbed molecular oxygen species participated in this reaction also.

The effect of partial pressures of propan-2-ol in the range 0.5-60 Torr upon the rate of photoassisted formation of acetone from propan-2-ol on ZnO was studied at a constant partial pressure of oxygen of 380 Torr. Outlined in fig. 6(*a*) are rates of acetone production plotted as a function of partial propan-2-ol pressure at reaction

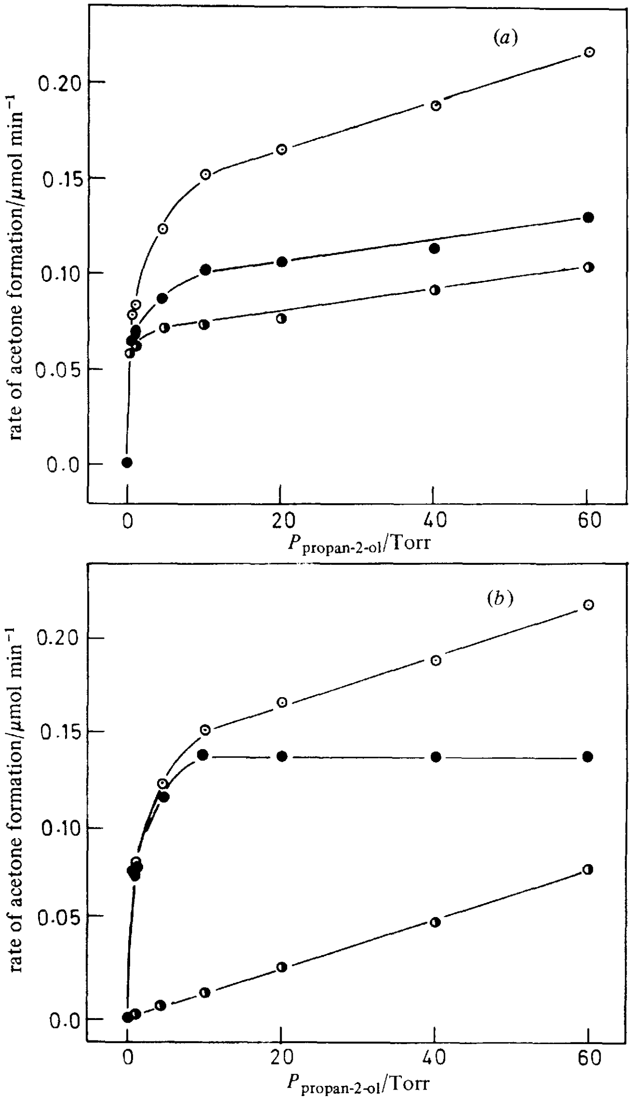

FIG. 6.—(*a*) Influence of partial pressure of propan-2-ol on rate of acetone production from propan-2-ol on ZnO measured after: (○) 5, (●) 25 and (◑) 125 min u.v. illumination. $M = 200$ mg, $P_{O_2} = 380$ Torr, $F = 40$ cm^3 min^{-1}. (*b*) Separation of overall rate of photoassisted production of acetone from propan-2-ol on ZnO measured after 5 min u.v. illumination into V_{LH} and V_{ER} components, as defined in eqn (3*a*) and (3*b*) in text.

times of 5, 25 and 125 min u.v. illumination. Attempts to linearise these data in terms of any one of several possible Langmuir–Hinshelwood type expressions (such as recently described by Pichat *et al.*[14] for photo-oxidation of ammonia over TiO_2) did not achieve satisfactory linear transformation. It was noticeable in all such attempts at linearization that the experimentally observed rates at higher alcohol pressures exceeded those predicted by LH expressions to progressively larger extents. A similar difficulty had previously been encountered by Thevenet *et al.*[15] in the dependence of rate of photo-oxidation of carbon monoxide on TiO_2 upon P_{CO} and led those workers to propose that the experimentally observed data arose from separate contributions by two photoassisted mechanisms to the overall rate of photo-oxidation. Similar deconvolution of the alcohol pressure dependence for overall rate in photoassisted conversion of propan-2-ol to acetone is illustrated in fig. 6(*b*). This shows that the data could be accounted for in terms of a LH*-type contribution, which dominated at low alcohol pressures, plus an ER*-type contribution increasing linearly with P_{ROH}. The latter contribution was readily distinguished by the linear increase in overall rate as P_{ROH} was increased above 20 Torr. Extrapolation of the linear segment to lower pressures and subtraction from the overall rate resulted in a residual component which was strongly non-linear but was found accurately to obey

$$P_{ROH}/\text{rate} = a + b\,P_{ROH}. \tag{2}$$

This kinetic behaviour of the second component corresponds well with what would be expected for a LH* process in which the θ_{ROH} term obeyed the Langmuir isotherm and attained its limiting value for $P_{ROH} \approx 10$ Torr. Thus, for a constant partial pressure of oxygen the overall rate of photoassisted production of acetone from propan-2-ol on ZnO may be described as in

$$V^*_{\text{total}} = V^*_{ER} + V^*_{LH} \tag{3a}$$

$$= k_{ER}P_{ROH} + \frac{k_{LH}P_{ROH}}{a + b\,P_{ROH}}. \tag{3b}$$

In the case of photoassisted production of acetaldehyde from propan-2-ol on ZnO a similar, but less pronounced, increase in rate of this reaction was observed at high alcohol pressures. Again a more satisfactory kinetic expression could be obtained by deconvolution of the overall reaction rate into two components, as represented by eqn (3*a*) and (3*b*).

The rate of photoassisted production of propene, which only appeared in trace quantities, was found to decrease with increasing oxygen pressure but appeared zero order in P_{ROH}.

(2) PULSED REACTANT PROCEDURE

(2*a*) GENERAL FEATURES OF PHOTO-OXIDATION IN PULSED REACTANT MODE

In order to study in more detail the decay in activity of the oxide surface with increasing extent of alcohol photodehydrogenation, the catalytic photoreactor was utilised in the pulsed-reactant mode [*cf.* fig. 1(*b*)]. Conditions were sought such that reaction(s) on the oxide surfaces would effectively be limited to the time taken for a reactant pulse to pass over the illuminated catalyst and be flushed out of the photoreactor onto the g.c. column for temperature-programmed separation. Ideally this would require that duration of illumination of the interface should coincide with transit time of the reactant pulse. Fig. 7(*a*) presents evidence that an approximation to this condition was achieved by commencing illumination of the oxide just 10 s prior to introduction of the reactant pulse and by continuing illumination for only another 60 s (which approximated to transit time through the photoreactor, as signalled by arrival of the end of the O_2 pulse at the g.c. detector). Fig. 7(*a*) illustrates how the amounts of acetone and acetaldehyde photoproducts, produced during passage of a reactant pulse through the photoreactor, increased for a (propan-2-ol+O_2)/ZnO* interface with increasing duration of u.v. illumination after introduction of a reactant pulse. Growth of the amount of acetaldehyde photoproduct levelled off at 90 s illumination time but data for acetone product in fig. 7(*a*) indicate that this product

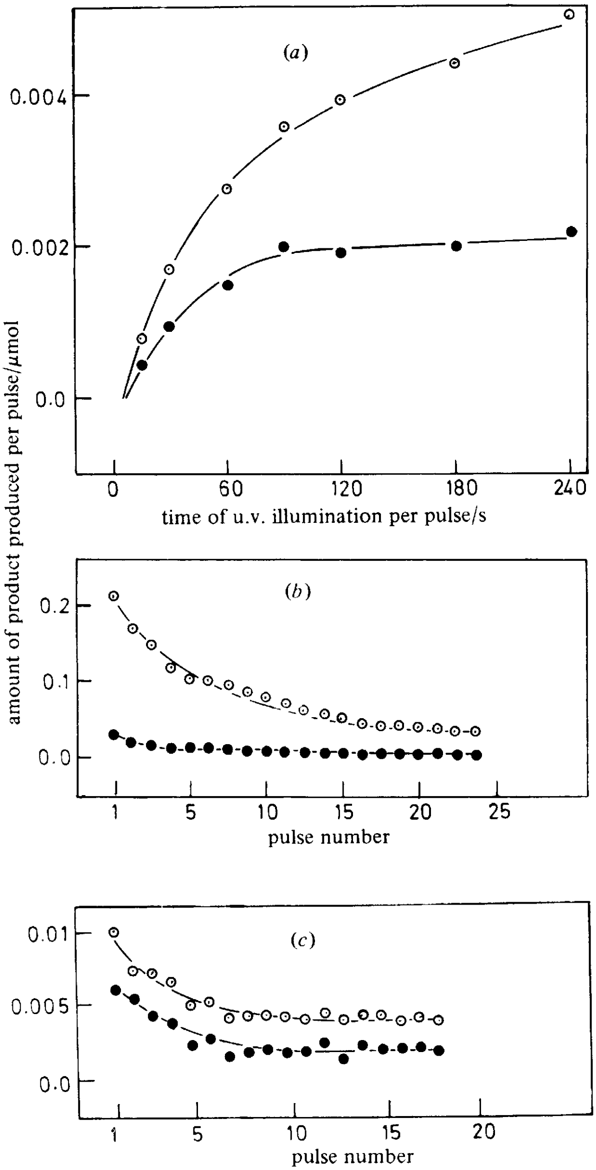

FIG. 7.—(*a*) Influence of time of u.v. illumination after injection of (propan-2-ol + O_2) reactant pulse on the amount of acetone (○) and acetaldehyde (●) produced from ZnO. $M = 50$ mg. Number of moles O_2 in pulse (N_{O_2}) = 10.4 μmol; number of moles propan-2-ol in pulse ($N_{\text{propan-2-ol}}$) = 0.55 μmol. (*b*) and (*c*) Amounts of acetone (○) and acetaldehyde (●) produced from (propan-2-ol + O_2) pulses on ZnO (*b*) and TiO_2 (*c*) plotted as a function of the total number of pulses passed over each surface. $M = 50$ mg, $N_{O_2} = 10.4$ μmol, $N_{\text{propan-2-ol}} = 0.55$ μmol.

increased for up to 240 s illumination, *i.e.* well after all gaseous oxygen had been flushed out of the photoreactor. A limitation of post-injection illumination to 60 s was adopted as the standard condition, since it appeared probable that undesirable reduction of the oxide surface by photoassisted reaction with adsorbed alcohol could accompany the additional acetone photoproduct attainable at illumination times 60-240 s after all gas-phase oxygen had been flushed out of the photoreactor. With the illumination duration limited to 70 s per pulse and an interval of 35 min allowed between successive pulses, the amount of acetone or acetaldehyde photoproducts from propan-2-ol on ZnO decreased with pulse number as illustrated in fig. 7(*b*). This shows a maximum conversion for the first reactant pulse, followed by diminishing intermediate values for pulse numbers 2-8 and with a reproducible extent of photocatalysed reaction finally being established for pulse numbers 9-20. Those results confirm that some decline in activity was an intrinsic feature of the u.v.-illuminated (propan-2-ol$+O_2$)/ZnO* interface, rather than some artifact associated with operation in the continuous reactant flow mode, a conclusion further strengthened by results shown in fig. 7(*c*) for a (propan-2-ol$+O_2$)/TiO* system, in the pulsed reactant mode. A marked decline is there evident in conversion per pulse, from a high value in the first pulse to intermediate and progressively decreasing values for pulses numbered $n = 2$ to 24 and eventually to a much reduced but effectively constant value for pulses > 30. Possibilities examined experimentally in seeking the origin of the observed decline in activity with increasing pulse number included: (i) blockage of some sites by other photoproducts such as CO_2 or other carbonaceous deposits; (ii) consumption of active surface oxygen species during photoassisted alcohol oxidation at rates exceeding their replenishment; (iii) irreversible dehydroxylation of sites rendered active initially by residual hydroxyls.

Carbon dioxide appeared a likely poison for the oxide surfaces since its formation as an important product of photoassisted reactions at (alcohol vapour$+O_2$)/TiO_2 surfaces had been directly measured.[5] Furthermore, ZnO surfaces of the type used in this study have been reported[16] to adsorb CO_2 so strongly in the dark that it was removed only upon heating to 623 K. Conversely the photodesorption of CO_2 in the presence of O_2 at lower temperatures had also been reported.[17, 18] A sequence of experiments was therefore carried out, first to determine the effects of preadsorbed CO_2 upon the type of decline in photocatalytic activity illustrated in fig. 7(*b*) for ZnO surfaces from pulse 1 to pulse 9, and secondly to establish if any such effects could be reversed by u.v. illumination.

Curve (i) of fig. 8(*a*) shows activity of a 'prereduced' ZnO surface which had been heated to 623 K in N_2 carrier gas to remove surface CO_2 from the 'as supplied' material. Curve (ii) shows that, when the prereduced ZnO surface was exposed to a flow of gaseous CO_2 at 348 K for 16 h prior to testing its photocatalytic activity towards a sequence of reactant pulses, the initial activity was greatly reduced, as also was the percentage decline in activity from pulses 1 to 9. These results show clearly that an accumulation of CO_2 or of CO_2-related surface species could account for much of the observed decline in activity from pulses 1 to 9. One possible objection to the relevance of data in fig. 8(*a*) to photoassisted reaction at (propan-2-ol$+O_2$)/ZnO* interfaces was that, in the presence of the gaseous oxygen component of each reactant pulse, the ZnO samples may not have been in a prereduced state but may rather have approximated to an oxidised state. To meet this objection rates of photoassisted conversion of propan-2-ol to acetone at 348 K were first measured over surfaces which had been preoxidised for 20 h in a stream of gaseous oxygen at 623 K and, secondly, measured after a similar preoxidation but followed by exposure to CO_2 for 16 h at 348 K. Comparisons of results from these measurements are shown on curves (i) and

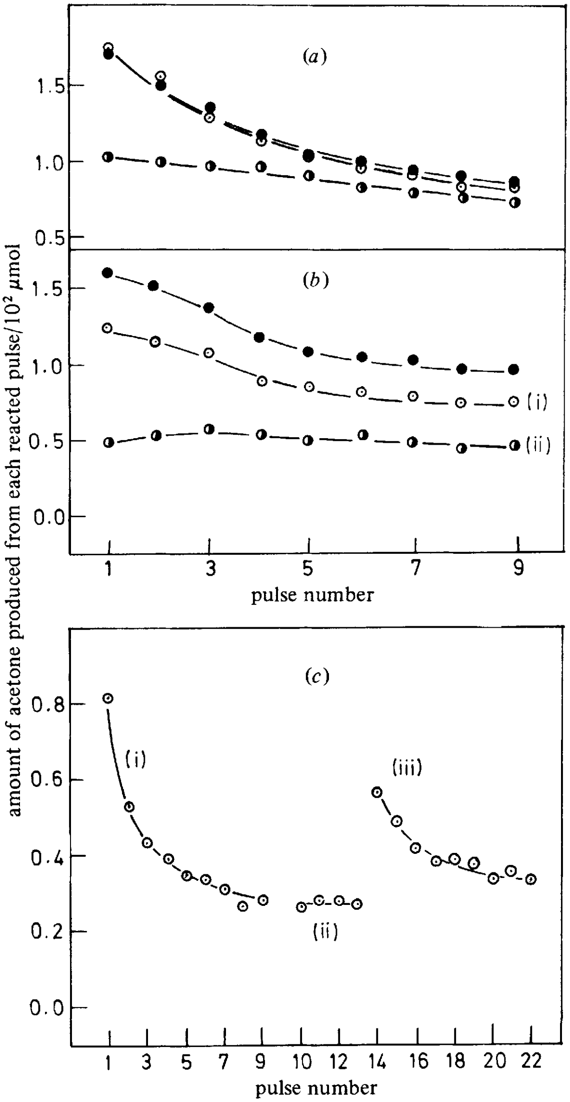

FIG. 8.—(*a*) and (*b*) Influence of pre-exposure of prereduced ZnO (*a*) and preoxidised ZnO (*b*) samples to $CO_2(g)$ (◑) at 348 K and to $H_2O(g)$ (●) at 623 K, on the amount of acetone produced from (propan-2-ol + O_2) pulses during passage through the photoreactor. The symbols (○) represent amount of acetone produced on prereduced or preoxidised ZnO samples not exposed to CO_2. (*c*) Influence of exposure of a ZnO sample to 30 pulses of gaseous oxygen (20.8 μmol per pulse) in the dark (ii) and with u.v. illumination (iii) on the activity of a ZnO sample which had previously declined from its initial activity level and had reached a photostationary state in (i). $M = 50$ mg, $N_{O_2} = 10.4$ μmol, $N_{\text{propan-2-ol}} = 0.55$ μmol.

(ii) of fig. 8(*b*) and demonstrate that the inhibiting effect of pre-adsorbed CO_2 upon an initially high photocatalytic activity was still clearly evident for the oxidised surface. This allows the conclusion that regardless of whether the ZnO surface was oxidised or reduced, an accumulation of CO_2-related species on these samples as photoassisted reaction proceeded could contribute to the observed decline in activity.

Reports that CO_2 could be photodesorbed from ZnO[17, 18] led to attempts to regenerate activity of reaction-poisoned surfaces. Some evidence that photoassisted reversal of the decline in catalytic activity was possible is summarised in fig. 8(*c*) which illustrates the effects of low-temperature treatments with various gases upon the activity of interfaces which previously had experienced an initial decline in activity and reached a photostationary state. Successive alcohol pulses, each comprised of 0.55 μmol propan-2-ol, fed to the partially poisoned (propan-2-ol + O_2)/ZnO* system at 30 s intervals either in the dark or with u.v. illumination (but in the absence of oxygen), were not successful in regenerating lost activity. Successive oxygen pulses in the dark, similarly, had no regenerative effect. However, admission of 30 pulses of oxygen, each pulse comprised of 20.8 μmol oxygen injected at 30 s intervals, in combination with continuous u.v. illumination for the time period for which the injections were made (15 min), had the effect of regenerating activity of the ZnO sample to the value shown in fig. 8(*c*). U.v. illumination in the absence of gas-phase oxygen did not regenerate lost activity.

Since some accumulation of chemisorbed or hydrogen-bonded H_2O species or of hydroxyl groups at the (propan-2-ol + O_2)/ZnO* surface also appeared a possible contributor to the decline in activity noted as photoassisted reaction proceeded, tests were made of the effects of pretreatment with water vapour upon activities of prereduced and preoxidised ZnO samples. Hydroxylation of the ZnO surfaces was carried out by passing water vapour ($P_{H_2O} \approx 15$ Torr) over these surfaces during the reduction or oxidation pretreatments at 623 K. Results presented as curves (i) and (iii) of fig. 8(*a*), showing identical activity for ZnO (red) surfaces which had or had not been exposed to water vapour, indicate that accumulation of H_2O-related species on the prereduced surface would not contribute to the initial decline in activity. By contrast, a slightly enhancing effect in catalytic activity was observed for exposure of preoxidised ZnO samples to water vapour, as is indicated by comparison of curves (i) and (iii) of fig. 8(*b*). This latter effect is reminiscent of the effects of hydroxylation on O_2/TiO_2[8, 19-23] and (propan-2-ol + O_2)/TiO_2*[2] systems.

Exposure of both prereduced and preoxidised ZnO samples to CO_2(g) had a similar inhibiting effect upon the rate of photoassisted production of acetaldehyde from (propan-2-ol + O_2) pulses. However, exposure of these surfaces to water vapour did not significantly affect the activity of these surfaces for this reaction.

Data illustrating the dependence of various parameters in the photoassisted conversion of propan-2-ol to acetone upon intensity of illumination are shown in fig. 9 for a ZnO catalyst. The curves in fig. 9(*a*) show how the amount of acetone produced from individual (propan-2-ol + O_2) pulses on ZnO varied with pulse number for differing values of illumination intensity. Comparison of the shapes of the curves at different intensities make it clear that the decline in conversion with increasing number of reactant pulses passed over the ZnO sample was more evident the higher the intensity of illumination. At the lower light intensities examined, the p.d.eq. was approached more rapidly from a lower initial activity level. The intensity dependence of the extent of photoassisted production of acetone is well represented in fig. 9(*b*) as linear plots of amounts of acetone produced during passage of the 9th reactant pulse through the photoreactor against the square root of the light intensity. For comparison, the former quantity is also plotted as a function of the first power of the intensity. Analysis of all data between the 1st and 9th reactant pulses also indicated that the amount of acetone produced per pulse was dependent upon $I^{\frac{1}{2}}$. In liquid alcohol/TiO_2* systems[24] similar dependence for rate of acetone production upon $I^{\frac{1}{2}}$ has been interpreted in terms of strong competition by processes involving recombination of photogenerated electrons and holes against processes which involve

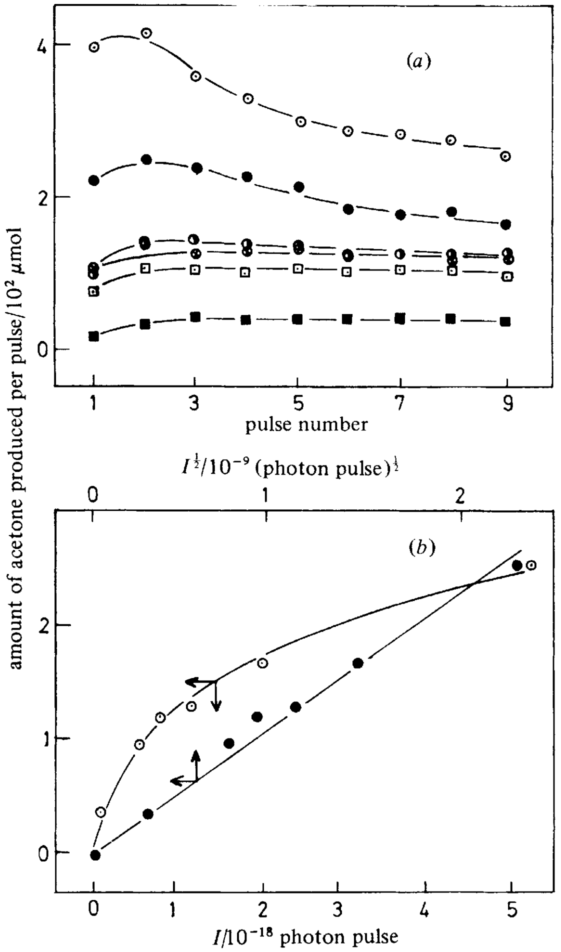

FIG. 9.—(*a*) Influence of u.v. illumination intensity on decay in catalytic activity for acetone production from (propan-2-ol+O_2) pulses over ZnO. $I = 5.3$ (○), 2.05 (●), 1.20 (⊗), 0.78 (◑), 0.55 (□), 0.08 (■) × 10^{18} photons per pulse. (*b*) Acetone production from 9th (propan-2-ol+O_2) pulse over ZnO plotted as a function of I (○) and $I^{\frac{1}{2}}$ (●). $M = 200$ mg, $N_{O_2} = 10.4$ μmol, $N_{\text{propan-2-ol}} = 0.55$ μmol.

participation of photogenerated holes in surface photo-oxidation. An additional consequence of the intensity dependence reported above is outlined in table 1 which shows an increase in relative quantum efficiency for acetone production from the 9th reactant pulse as illumination intensity was decreased. This increase in efficiency as illumination intensity decreased would be consistent with increased competition from electron–hole recombination as intensity increased.[24] The quantum efficiencies presented in table 1 are quoted as relative values because no attempt was made to optimise these efficiencies by such procedures as increasing the reactant pulse size. Additionally these values were estimated on the basis that all irradiation absorbed by the actiometer solutions was also absorbed by the ZnO catalyst and was capable of affecting photoassisted conversion of alcohol to ketone product. In reality, studies of the wavelength dependence of the photoassisted oxidation confirmed that photons of energy greater than the band-gap of ZnO, *i.e.* < 400 nm, were necessary whereas

TABLE 1.—PHOTOASSISTED PRODUCTION OF ACETONE AND ACETALDEHYDE FROM PROPAN-2-OL ON ZnO IN PULSED REACTANT FLOW OPERATION. RELATIVE QUANTUM EFFICIENCIES FOR PRODUCT FORMATION DURING PASSAGE OF PULSE THROUGH THE PHOTOREACTOR AT THE U.V. ILLUMINATION INTENSITIES INDICATED.

intensity (10^{-16} × no. of photons entering reactor per s)	$\phi_{\text{acetone}} \times 10^3$	$\phi_{\text{acetaldehyde}} \times 10^4$
7.6	2.9	4.7
2.9	4.9	6.7
1.7	6.5	6.1
1.1	9.3	7.3
0.78	10.4	8.3
0.12	26.4	27

The quantum efficiencies in this table were calculated on the basis that all irradiation entering the reactor in the wavelength range 300-500 nm was absorbed by the catalyst.

the actinometer solution was sensitive to light in the wavelength range 300-500 nm. Since the maximum improvement attainable through correction for these factors was a five-fold increase, it was clear the $(-H_2)^*$ was a rather inefficient process at high intensities.

Analysis of data pertaining to photoassisted production of acetaldehyde from (propan-2-ol + O_2) pulses passed over ZnO at various u.v. illumination intensities indicated that the amount of acetaldehyde produced per pulse depended upon the first power of the intensity. Relative efficiencies of $(\alpha-\beta)^*$ at various illumination intensities are quoted in table 1 and again this process appears rather inefficient at high light intensities.

(2*b*) PRESSURE DEPENDENCE OF PHOTOASSISTED REACTIONS IN PULSED REACTANT MODE

Dependence of photocatalytic activity at the (propan-2-ol + O_2)/ZnO* interface upon the amounts of alcohol or oxygen reactants present in each pulse was investigated in the pulsed reactant mode by using conversion at p.d.eq. (*i.e.* at pulse numbers > 9) as a relative measure of reproducible catalytic activity. Fig. 10 summarises data illustrating the dependence of activity for $(-H_2)^*$ and $(\alpha-\beta)^*$ processes (at a constant alcohol content per pulse of 0.55 μmol) upon N_{O_2}, moles of the oxygen component in the range 0-20 μmol introduced to the photoreactor. Kinetic analysis of these data could be carried out by eqn (1), provided it was assumed that the actual pressure of reactants over the oxide surface was directly related to the amount introduced per pulse by a proportionality constant *kp* in an expression such as [pressure of reactant(s) over surface] = *kp* × [amounts of reactant(s) pulsed]. When these data were plotted according to just such a modified version of eqn (1), *i.e.* $N_{O_2}/\text{rate} = a + bN_{O_2}$, the linearity of these plots for acetone and acetaldehyde photoproducts appeared consistent with a process whereby the reaction rates were related to the surface coverage by adsorbed molecular oxygen, whose concentration in turn was governed by the Langmuir equation for adsorption of O_2 without dissociation at the (O_2 + alcohol)/ZnO interface.

The effects of varying the amount of propan-2-ol present in each pulse in the range 0.025-1.65 μmol, at a constant N_{O_2} = 10.4 μmol, upon the amounts of acetone and

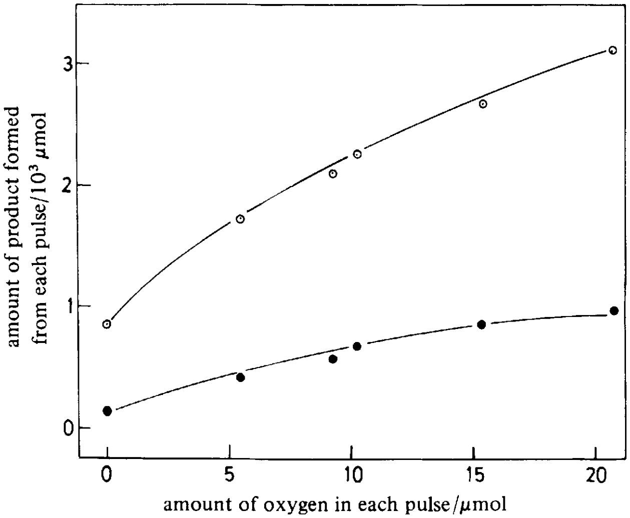

FIG. 10.—Influence of amount of oxygen in each pulse on amount of acetone (○) and acetaldehyde (●) produced from propan-2-ol on ZnO.

acetaldehyde produced per pulse, were examined for a ZnO sample which had reached p.d.eq. and are outlined in fig. 11(*a*). The behaviour of the rate of photoassisted production of acetone showed a striking similarity to the behaviour reported above for the analogous effect in the 'continuous reactant flow' (*cf.* fig. 6). Note again that the rate of photoassisted production of acetone did not level off to a constant value when large amounts of alcohol were pulsed but showed rather a continuing increase in reaction rate as the amount of alcohol pulsed was further increased. After taking into account the assumption regarding proportionality between alcohol introduced in the pulse and the actual pressure over the metal oxide catalyst, it was found that kinetic expressions of the type outlined in eqn (2) were inadequate to represent the collected data, since deviations were observed from behaviour characterised by such expressions for large amounts of alcohol pulsed. Outlined in fig. 11(*b*) is a more successful kinetic analysis which involved an assumption already discussed above, that two separate reaction mechanisms were contributing to the overall amounts of acetone produced. Thus the overall amounts of acetone produced from (propan-2-ol+O_2) pulses over ZnO could be represented by appropriately modified versions of eqn (3*a*) and (3*b*).

The amounts of acetaldehyde produced from each reactant pulse are plotted as a function of the size of the propan-2-ol component of the pulse as the lower trace of fig. 11(*a*). However, amounts of acetaldehyde produced were not sufficiently large to allow for confident determination of whether an Eley–Rideal-type component for this reaction existed in the 'pulsed reactant flow' mode, such as would be consistent with the small Eley–Rideal-type component that was observed for this product in 'continuous reactant flow' mode.

(2*c*) COMPARISONS OF RESULTS IN 'PULSED REACTANT' AND 'CONTINUOUS FLOW' CONDITIONS

An important aspect of the foregoing results is the good agreement achieved between observations made using the 'continuous reactant flow' and 'pulsed reactant

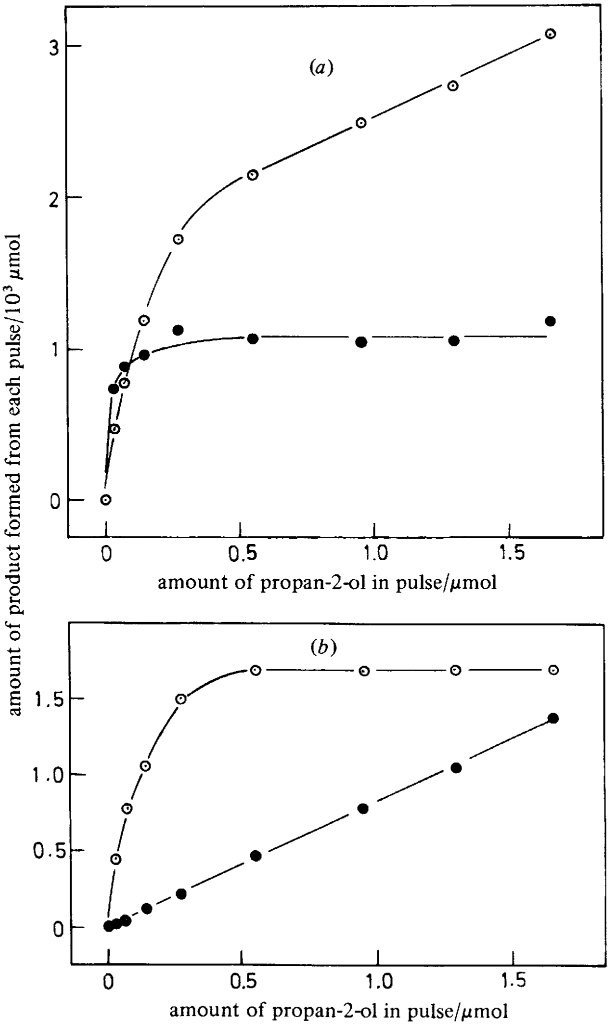

FIG. 11.—(*a*) Influence of size of the propan-2-ol component of the reactant pulse on the amounts of acetone (○) and acetaldehyde (●) produced on ZnO. (*b*) Separation of the total amounts of acetone produced from the upper curve of part (*a*) of the figure into V_{ER} (●) and V_{LH} (○) components of eqn (3*a*) and (3*b*) of text. $M = 50$ mg, $N_{O_2} = 10.4$ μmol.

flow' modes of operation. Data presented above, particularly those pertaining to measurements of apparent activation energies for $(-H_2)^*$ and $(\alpha-\beta)^*$ reactions in the system (butan-2-ol$+O_2$)/TiO_2^* and to the influence of reactor loading for reaction rates measured at identical times after commencement of u.v. illumination, provide valuable empirical evidence to support the proposal that meaningful study of reaction parameters was possible not only in p.d.eq. but also in non-p.d.eq. situations, provided that the conversions compared had been measured at identical times after commencement of u.v. illumination. Thus it can be argued that observed extents of conversion by the $(-H_2)^*$ process in the system (propan-2-ol$+O_2$)/ZnO* (*cf.* fig. 6) at varying alcohol pressures, as measured at identical times after commencement of u.v. illumination, reflect genuine kinetic parameters of the photoassisted process for the reaction times indicated and were not an artifact of the measurement technique used. Furthermore, the success of the same kinetic analysis for data measured in 'continuous flow' and 'pulsed reactant flow' modes, and the observation that catalytic decay was prevalent with both experimental procedures, provide strong experimental support for two significant qualitative conclusions: first, that an initial decline in activity of the ZnO and TiO_2 surfaces undoubtedly occurred at high u.v. illumination intensities with the extent of alcohol photo-oxidation thereon, to be succeeded by a stable level of photodynamic activity and secondly, that dependence of rate of $(-H_2)^*$ for the system (propan-2-ol$+O_2$)/ZnO* cannot be as well-fitted by any single steady-state kinetic expression as by assuming that the overall reaction rate represented the sum of two individual processes as represented by eqn (3*a*) and (3*b*). The observations that a maximum was observed in rate of $(-H_2)^*$ and $(\alpha-\beta)^*$ reactions for the system (propan-2-ol$+O_2$)/ZnO* in the 'continuous reactant flow' mode, whereas no such maximum was detectable in the 'pulsed reactant flow' mode, could be understood on the basis of differing real pressures over the illuminated sample. Thus whilst partial pressure of reactants introduced into the pulse volume of 0.5 cm^3 was comparable to that present over the ZnO catalyst in the continuous mode, expansion of this volume into the larger volume of the reactor resulted in considerable lessening of the effective reactant pressure experienced by the catalyst sample.

DISCUSSION

Present observations confirm and reinforce the conclusions drawn by previous workers[2,5] that if continuing photocatalysed oxidation of alcohol is to be observed on ZnO or TiO_2 surfaces then the following factors must simultaneously be present at the interface: u.v. photons inside the band edge of the metal oxide, gaseous oxygen and alcohol vapour. Overall mechanisms intending to account for these general features of alcohol photo-oxidation on ZnO and TiO_2 should ideally take into account the following elementary processes which are possible within these n-type semiconductors or at the interface between them and the (alcohol$+O_2$) reactant.

DARK PROCESSES

Equilibration of electrons between surface and bulk

$$e_b^- \rightleftharpoons e_s^-. \tag{D 1}$$

Electron localization by adsorbed oxygen

$$e_s^- + O_2\,(\text{ads}) \rightleftharpoons O_2^-\,(\text{ads}). \tag{D 2}$$

Adsorption in uncharged forms

$$O_2\,(\text{g}) \rightleftharpoons O_2\,(\text{ads}) \tag{D 3}$$

$$>\text{CHOH}\,(\text{g}) \rightleftharpoons\, >\text{CHOH}\,(\text{ads}). \tag{D 4}$$

Formation of weak donor–acceptor surface complexes

$$>\text{CHOH}\,(\text{ads}) + O_2^- \rightleftharpoons [>\text{CHOH}{-}{-}{-}O_2]^-(\text{ads}) \tag{D 5}$$

$$>\text{CHOH}\,(\text{ads}) + O_2 \rightleftharpoons [>\text{CHOH}{-}{-}{-}O_2](\text{ads}). \tag{D 6}$$

PHOTOELECTRONIC PROCESSES UNDER U.V. ILLUMINATION

Photogeneration of electron–hole pairs

$$\mathrm{MO} + h\nu \rightleftharpoons \mathrm{e}^- + \mathrm{h}^+. \tag{U 1}$$

Hole migration to and localization at the interface

$$\mathrm{h}^+ + \mathrm{O}^{2-}_{\mathrm{cus}} \rightarrow \mathrm{O}^-_{\mathrm{cus}} \tag{U 2}$$

$$\mathrm{h}^+ + \mathrm{O}_2^-\,(\mathrm{ads}) \rightarrow \mathrm{O}_2^* \tag{U 3}$$

$$\mathrm{h}^+ + \,>\!\mathrm{CHOH}\,(\mathrm{ads}) \rightarrow \,>\!\mathrm{CHOH}^+\,(\mathrm{ads}) \tag{U 4}$$

$$\mathrm{h}^+ + [>\!\mathrm{CHOH}{-}{-}{-}\mathrm{O}_2]^- \rightarrow [>\!\mathrm{CHOH}{-}{-}{-}\mathrm{O}_2]^*. \tag{U 5}$$

SURFACE REACTIONS OF PHOTOACTIVATED SPECIES

$$\mathrm{O}^-_{\mathrm{cus}} + \mathrm{O}_2 + \,>\!\mathrm{CHOH} \rightarrow \,>\!\mathrm{CO} + \mathrm{OH}^-_{\mathrm{s}} + \mathrm{HO}_2 \tag{S 1}$$

$$\mathrm{O}^-_{\mathrm{cus}} + [>\!\mathrm{CHOH}{-}{-}{-}\mathrm{O}_2] \rightarrow \,>\!\mathrm{CO} + \mathrm{OH}^-_{\mathrm{s}} + \mathrm{HO}_2 \tag{S 2}$$

$$\mathrm{O}_2^* + \,>\!\mathrm{CHOH} \rightarrow \,>\!\mathrm{CO} + \mathrm{H}_2\mathrm{O}_2 \tag{S 3}$$

$$(>\!\mathrm{CHOH})^+ + \mathrm{O}_2^- \rightarrow \,>\!\mathrm{CO} + \mathrm{H}_2\mathrm{O}_2 \tag{S 4}$$

$$(>\!\mathrm{CHOH})^+ + \mathrm{e}^-_{\mathrm{s}} \rightarrow (>\!\mathrm{CHOH})^*. \tag{S 5}$$

REGENERATION OF PHOTOCATALYTIC SITES

$$\mathrm{OH}^-_{\mathrm{s}} + \mathrm{HO}_2^- \rightarrow \mathrm{O}^{2-}_{\mathrm{cus}} + \mathrm{H}_2\mathrm{O}_2 \tag{R 1}$$

The primary objectives of the following kinetic analysis are (i) the identification of which of these possible elementary processes exert an important rate-determining influence on the observed $(-H_2)^*$ photoreaction and (ii) the incorporation of these processes into physically reasonable overall mechanisms for the $(-H_2)^*$ process.

Data on the dependence of rate of the $(-H_2)^*$ process upon P_{O_2} at relatively low fixed alcohol pressure (*cf.* fig. 5 and 10) and upon P_{ROH} over a range of low alcohol pressures with fixed oxygen pressure (*cf.* fig. 6 and 11) point to the involvement of the terms θ_{O_2} and θ_{ROH} in the rate expression. Taken together with the observed dependence of conversion upon $I^{\frac{1}{2}}$ this leads to

$$\mathrm{d}(-\mathrm{H}_2)/\mathrm{d}t = k_{(-\mathrm{H}_2)}\theta_{\mathrm{O}_2}\theta_{\mathrm{ROH}}I^{\frac{1}{2}} \tag{4}$$

as an overall rate expression for $(-H_2)$.*

Dependence of rate upon $I^{\frac{1}{2}}$ can be understood on the basis: (i) that the photoassisted process requires photoactivation of a surface species [*cf.* eqn (U 2)-(U 5)] through localization of a photogenerated hole and (ii) that the concentration of such holes reaching the surface is but a small fraction of those produced by I_{abs}, the remainder disappearing by rapid electron–hole recombination, *i.e.* the reverse of eqn (U 1). The steady-state approximation for free hole concentration may be further simplified to $I_{\mathrm{abs}} \approx k_{(-\mathrm{U}\,1)}[\mathrm{e}^-][\mathrm{h}^+] \approx k_{(-\mathrm{U}\,1)}[\mathrm{h}^+]^2$ in high intensity conditions such that most photogenerated holes recombine with photogenerated electrons rather than with the dark concentration of electrons. In this limit,[24] $[\mathrm{h}^+]$ becomes proportional to $I^{\frac{1}{2}}$, so that processes which depend on $[\mathrm{h}^+]$ should vary with $I^{\frac{1}{2}}$. Support for the idea that surface photoreactions were in competition with efficient electron–hole recombination comes from the low quantum efficiencies observed at high intensities (*cf.* table 1).

Arrival at the illuminated interface of that small fraction of photogenerated holes which escape rapid hole–electron recombination thus represents the driving force of the $(-H_2)^*$ process. Eqn (4) indicates that the surface coverage terms, θ_{O_2} and θ_{ROH}, also exert a controlling influence on the attainable rates. Furthermore, the agreements noted in the Results section between dependence of rate upon P_{O_2} or P_{ROH} and θ_{O_2} or θ_{ROH} expressions, assuming non-dissociative adsorption, emphasise the involvement of non-dissociatively adsorbed oxygen and alcohol species in the r.d.p. Formally the simplest processes capable of meeting these requirements would be direct localization of a hole by a non-dissociatively adsorbed oxygen or alcohol species [*cf.* eqn (U 3) and (U 4)] and subsequent reaction of the photoactivated O_2^* or $>$CHOH$^+$ species thereby produced [*e.g.* *via* surface reactions (S 3) or (S 4)]. Independent evidence is lacking, however, that singlet molecular oxygen can dehydrogenate ground-state alcohols[25] or that $(-H_2)$ would be the preferred product from eqn (S 4). Good evidence does exist, however, that O$^-$-type species selectively abstract α-hydrogens from secondary or primary alcohols.[26, 27] Consequently, photoactivation of a surface lattice oxide ion by hole capture [*cf.* eqn (U 2)], followed by interaction of the resultant O_s^- species *via* eqn (S 1) with adsorbed alcohol and adsorbed O$_2$,[4] or *via* eqn (S 2) with a weak [alcohol---O$_2$] surface complex, merit consideration as alternative r.d.p. capable of giving rate expressions of the form of eqn (4). It can readily be shown[28] that the inclusion of the surface concentration of O_{cus}^-, θ_{O^-}, in rate expressions for the elementary processes (S 1) or (S 2) leads to a dependence upon [h$^+$] and so to an $I^{\frac{1}{2}}$ dependence, and that dependence upon θ_{O_2} or θ_{ROH} would arise indirectly from eqn (S 1) or from eqn (S 2) *via* equilibria (D 5) or (D 6). A role of such complexes has recently been envisaged in electrochemical oxidation of alcohols.[29]

A mechanism based on eqn (U 2) plus eqn (S 1) or (S 2) can also account for the convincing experimental evidence that an LH* component dominated the $(-H_2)^*$ process at lower alcohol pressures whereas an ER* component became increasingly important at higher alcohol pressures [*cf.* fig. 6 and 11 and also eqn (3*a*) and (3*b*)]. Since it is widely considered that oxide ions will exist on the powdered metal oxide surfaces with varying degrees of coordinative unsaturation,[30] various strengths of alcohol adsorption can be expected, ranging from strong irreversible adsorption onto highly coordinatively unsaturated O_{cus}^{2-} sites to weak reversible adsorption onto 'normal' surface lattice oxide ions, O_s^{2-}. Alcohol adsorption onto the O_{cus}^{2-} sites could be expected to lead to an LH* component at low alcohol pressures, since θ_{ROH} on these O_{cus}^{2-} sites should be greater than on O_s^{2-} and should reach saturation coverage of the O_{cus}^{2-} sites at low pressures. The behaviour deduced for the V_{LH} component is fully consistent with these ideas and indicates that eqn (U 2) plus (S 1) may be more adequately represented by the following scheme:

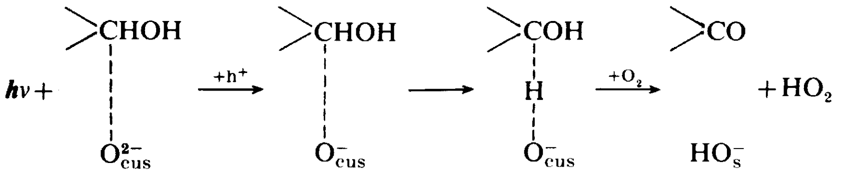

(A)

This scheme makes it clear that the LH* component has more the character of a biomolecular process than a three-body process, as eqn (S 1) might suggest. The evidence given in fig. 5 that $(-H_2)^*$ passed through a maximum and declined as P_{O_2} was increased to high values may be understood on the basis of competition by O$_2$

against ROH for adsorption on the O^{2-}_{cus} sites.[31] Compared with adsorption onto O^{2-}_{cus} sites, the weak reversible adsorption of alcohol onto normal surface lattice oxygen could be expected to yield much lower coverage of these sites at low alcohol pressures. However, the greater number of such normal O^{2-}_{s} sites offers possibilities for θ_{ROH} on such sites to continue to increase after saturation of the O^{2-}_{cus} sites. This would account for the V_{ER} component of the $(-H_2)^*$ process. Visualised in this manner the V_{ER} component is very similar to scheme (A) above, except that O^{2-}_{s} replaces O^{2-}_{cus} and that the alcohol is much less strongly held. Difficulties arise in attempting to distinguish on the basis of purely kinetic data between such surface reactions involving a weakly held molecular species and the case where the molecular species collides from the gas phase with an activated surface species or location.[31] Mechanisms of the latter type usually would be termed Eley–Rideal but it will be clear from the foregoing that this title must not here be interpreted as excluding scheme (A) involving photoactivation of alcohol weakly adsorbed on O^{2-}_{s} sites. It should also be noted that, in contrast with the success achieved in accounting for the pressure dependence of the $(-H_2)^*$ process on the basis of LH* and ER* variation of scheme (A), no satisfactory explanation of eqn (4) could be achieved with models of the Mars and Van Krevelen[32] type (involving only lattice oxygen as the oxidant) or of the SSA type (involving molecular oxygen not in equilibrium with the surface).[33, 34]

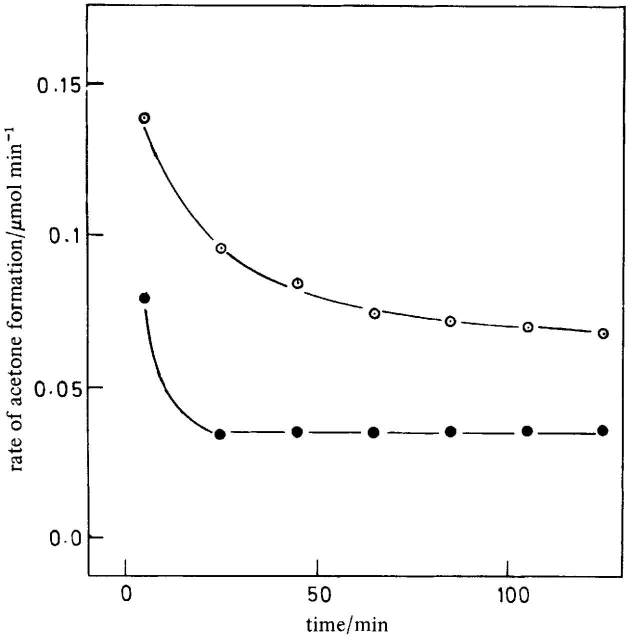

FIG. 12.—Separated contributions by Langmuir–Hinshelwood (○) and Eley–Rideal (●) type processes to the overall rate of acetone formation from (propan-2-ol + O_2)/ZnO* system. $M = 200$ mg, $P_{O_2} = 380$ Torr, $P_{\text{propan-2-ol}} = 60$ Torr.

The foregoing discussion of Langmuir–Hinshelwood and Eley–Rideal type components left unresolved the origin of the decay in rate of $(-H_2)^*$ with extent of that reaction. The question of whether such decay originated from one or from both Langmuir–Hinshelwood and Eley–Rideal components was examined by kinetic analysis [at various reaction times after starting $(-H_2)^*$ in the system (propan-

2-ol + O_2)/ZnO*] of the alcohol pressure dependence in the 'continuous reactant flow' mode. Such analysis involved, first, an estimation of the Eley–Rideal component of the overall reaction rate by extrapolation of the linear segment of the alcohol pressure dependence plots, constructed from data all measured at the same reaction time, secondly, assignment of the balance of the total activity to the Langmuir–Hinshelwood process and, thirdly, plotting for a selected alcohol pressure (60 Torr), the manner in which the Langmuir–Hinshelwood and Eley–Rideal components varied for different reaction times. Results of the analysis are shown in fig. 12 and clearly indicate that the decay in activity at reaction times in excess of *ca.* 20 min originated predominantly from the Langmuir–Hinshelwood component. This greater susceptibility of the LH* component towards deactivation as reaction proceeds appears fully consistent with involvement of O^{2-}_{cus} in the process.

Consideration of the factors which were likely to cause decay in activity at reaction times in excess of *ca.* 20 min can thus be limited to those likely to affect the Langmuir–Hinshelwood component, *e.g.* the rates of adsorption and desorption on O^{2-}_{cus} sites. The rate of evolution into the gas phase of detectable products of photoassisted oxidation of alcohols on ZnO and on TiO_2 fell instantaneously to zero when u.v. illumination was stopped and this finding could be interpreted within the framework of the transient response theory as indicating that desorption of these major products was not a slow process.[35] Rather, that theory would suggest that the initially high but decaying time profiles for product formation originated from an accumulation of adsorbed alcohol on these surfaces during dark exposure to reactants, with initial rate of consumption by photo-oxidation reactions being greater than the subsequent rate of regeneration by an adsorption process. This, however, cannot represent a complete explanation of the catalytic decay behaviour, since the decay was observed in the pulsed reactant flow mode irrespective of whether or not the photocatalysts were exposed to reactant pulses in the dark prior to u.v. illumination with subsequent pulses. Failure to regenerate catalytic activity by exposure of the catalysts to an excess of reactants (*cf.* fig. 8) can be taken as further evidence that the decay in photoactivity did not stem purely from slow alcohol adsorption. Other possibilities were: (i) that the observed decay in activity may have been caused by inhibition of the alcohol adsorption process through accumulation of some slowly desorbing surface poison such as CO_2 formed in the photo-oxidation process and (ii) that electronic factors such as the degree of band-bending at the surface were altered slowly by continuing illumination and resulted in decline of the efficiency of arrival of holes at the surface. Evidence that pre-adsorbed CO_2 caused a decline in surface activity was presented above and would be consistent with poisoning of O^{2-}_{cus} sites through formation of CO_3^{2-} surface species by reaction with CO_2 photoproducts from alcohol photo-oxidation.[5] The literature suggests not only that this reaction can be accelerated[16] by u.v. illumination in the presence of CO_2, but also that it can be reversed[17, 18] under illumination in the presence of O_2, and such behaviour provides a basis for understanding the observations made here on decay and regeneration of surface activity (*cf.* fig. 8). Mention may also be made here of other specific poisoning studies showing that pre-adsorption of other poisons likely to attack the strongly basic O^{2-}_{cus} sites, such as acetic acid or phenol, also inhibited alcohol adsorption and photo-oxidation.[1]

Although it is clear from the results given here that the photoassisted $(\alpha{-}\beta)^*$ process was of comparable efficiency to that for the $(-H_2)^*$ process, detailed discussion of the $(\alpha{-}\beta)^*$ process will be deferred to a later paper,[1] together with considerations of the role of surface hydroxyl, HO_2 and H_2O_2 species.

A maintenance grant (for B.K.H.) from the Department of Education of the Irish Government during part of this study is acknowledged together with valuable discussions with Professors R. B. Cundall and H. Knözinger and Dr Pierre Pichat.

[1] J. Cunningham and B. K. Hodnett, *J. Chem. Soc., Faraday Trans. 1*, to be published.
[2] R. I. Bickley, G. Munuera and F. S. Stone, *J. Catal.*, 1973, **31**, 398.
[3] M. Formenti, F. Juillet and S. J. Teichner, *Bull. Soc. Chim. Fr.*, 1976, 1631.
[4] J. Cunningham, B. K. Hodnett and A. Walker, *Proc. R. Ir. Acad.*, 1977, **77**, 411.
[5] A. Walker, M. Formenti, P. Meriandeau and S. J. Teichner, *J. Catal.*, 1977, **50**, 237.
[6] J. Cunningham, D. J. Morrissey and E. L. Goold, *J. Catal.*, 1978, **53**, 68.
[7] J. Cunningham, E. Finn and N. Samman, *Faraday Discuss. Chem. Soc.*, 1974, **58**, 160.
[8] R. I. Bickley and R. K. M. Jayanty, *Faraday Discuss. Chem. Soc.*, 1974, **58**, 194.
[9] S. Kubota, M. Iwaizumi and T. Isobe, *J. Phys. Chem.*, 1973, **77**, 2837.
[10] N. Takezawa and H. Kobayashi, *J. Catal.*, 1972, **25**, 179.
[11] H. Knözinger and B. Stubner, *J. Phys. Chem.*, 1978, **82**, 1526.
[12] J. Cunningham, B. Doyle and E. Leahy, *J. Chem. Soc., Faraday Trans. 1*, 1979, **75**, 2000.
[13] N. Ojerhri, M. Formenti, F. Juillet and S. J. Teichner, *Faraday Discuss. Chem. Soc.*, 1974, **58**, 185.
[14] H. Mozzanega, J-M. Herrmann and P. Pichat, *J. Phys. Chem.*, 1979, **83**, 2251.
[15] A. Thevenet, F. Juillet and S. J. Teichner, *Proc. 2nd Int. Conf. Solid Surfaces, Jpn J. Appl. Phys.*, 1974, suppl. **2**, 529.
[16] H. Chon and C. D. Prater, *Faraday Discuss. Chem. Soc.*, 1966, **41**, 380.
[17] Y. Shapira, R. B. McQuistan and D. Lichtman, *Phys. Rev.*, 1977, **15**, 15.
[18] Y. Shapira, S. M. Cox and D. Lichtman, *Surf. Sci.*, 1976, **54**, 43.
[19] R. I. Bickley and F. S. Stone, *J. Catal.*, 1973, **31**, 389.
[20] A. H. Boonstra and C. A. H. A. Mutsaers, *J. Phys. Chem.*, 1975, **79**, 1694.
[21] A. H. Boonstra and C. A. H. A. Mutsaers, *J. Phys. Chem.*, 1975, **79**, 1940.
[22] G. Munuera, V. Rives-Arnau and A. Saucedo, *J. Chem. Soc., Faraday Trans. 1*, 1979, **75**, 736.
[23] A. R. Gonzalez-Elipe, G. Munuera and J. Soria, *J. Chem. Soc., Faraday Trans. 1*, 1979, **75**, 748.
[24] T. A. Egarton and C. J. King, *J. Oil Colour Chem. Assoc.*, 1979, **62**, 386.
[25] D. R. Kearns, *Chem. Rev.*, 1971, **71**, 35.
[26] J. M. Warman, *J. Phys. Chem.*, 1968, **72**, 52.
[27] P. Neta and R. J. Schuler, *J. Phys. Chem.*, 1975, **79**, 1.
[28] B. K. Hodnett, *Ph.D. Thesis* (National University of Ireland, 1980).
[29] M. Miyake, H. Yoneyama and H. Tamura, *J. Catal.*, 1979, **58**, 22.
[30] S. R. Morrison, *Surf. Sci.*, 1975, **50**, 329.
[31] S. L. Bernasek and G. A. Somorjai, *J. Chem. Phys.*, 1975, **62**, 3149.
[32] P. Mars and D. W. Van Krevelen, *Chem. Eng. Sci.*, 1954, **3**, 41.
[33] K. A. Shelstad, J. Downie and W. F. Graydon, *Can. J. Chem. Eng.*, 1961, **38**, 102; 1962, **39**, 201.
[34] J. A. Juusola, R. F. Mann and J. Downie, *J. Catal.*, 1970, **17**, 106.
[35] H. Kobayashi and M. Kobayashi, *Catal. Rev.*, 1975, **10**, 139.

(PAPER 0/1859)